Investigating the role of calibration of hygrothermal simulations in the low carbon retrofit of solid walls

YUANSONG DING MSC
UCL Institute for Environmental Design and Engineering, University College London, London (UK)
zczlyd4@ucl.ac.uk

DR VALENTINA MARINCIONI ENGD
UCL Institute for Environmental Design and Engineering, University College London, London (UK)
v.marincioni@ucl.ac.uk

ANNE SCHMIDT
Historic Environment Scotland, Edinburgh ((UK)
anne.schmidt@hes.scot

ROGER CURTIS MRICS
Historic Environment Scotland, Edinburgh ((UK)
roger.curtis@hes.scot

Abstract
Solid masonry buildings account for around 20% of the UK building stock. As a traditional building material in the UK, stone could enhance the architectural style of buildings and last for thousands of years. However, historic buildings inevitably face the issue of diminished performance over hundreds or thousands of years. For these historic buildings whose appearance is protected, internal wall insulation (IWI) is a possible solution for protecting the façade while saving energy, improving indoor thermal comfort, and reducing carbon emissions. Of concern is that IWI could alter the drying capacity of the structure, thereby increasing moisture accumulation and causing durability issues such as freeze-thaw damage and mould growth. Hygrothermal simulations is one of the most commonly used methods to compare the performance and feasibility of different IWI assemblies. However, an inadequate assessment could lead to the specification of inappropriate IWI, prompting an incorrect choice of retrofit strategy. This study investigates the role of calibration in the assessment of moisture risks and durability of a solid masonry wall. The calibration of a hygrothermal model was performed using in-situ monitoring data; the model can be used for the comparison of IWI systems. According to the results, the selection of material properties had the highest impact in the calibration.

Keywords Calibration; Historic Buildings; Internal Wall Insulation; Hygrothermal Simulations; Solid Walls

1 Background
Buildings contribute approximately to 30% of total global energy consumption (1) and to 30% of global carbon emissions (2). Moreover, in UK, new buildings are a small fraction (1%) of the building stock each year (3). Most historic buildings in the UK are constructed with stone or brick walls. Masonry buildings account for 20% of the UK building stock. 92% of solid wall buildings were not insulated as of 2016 in the UK,

which suggest poorer energy efficiency compared to other building types (4, 5) and a high potential for improvement.

Buildings are significantly affected by climate in many ways. Wind-driven rain (WDR) exerts a horizontal force on the building envelope and promotes rain and moisture penetration into the exterior wall structure (6). Due to precipitation and wind, masonry walls can be subject to surface damage, cracking and peeling (7, 8).

For historic stone buildings, internal wall insulation (IWI) may be the only strategy to improve energy efficiency while maintaining the appearance and geometry. However, certain insulation materials affect the balance between air and water movement, which reduces the drying capacity of the structure and increases the probability of moisture accumulation. Moisture accumulation inside the exterior walls could cause freeze-thaw damage, salt crystallisation, and mould growth, making moisture one of the most critical issues affecting the structure of masonry buildings and the health of their occupants. Furthermore, moisture can be detrimental to the thermal insulation of materials (9), which negatively affects energy use and indoor thermal comfort. In response to these issues, the retrofit of historic masonry buildings on the exterior walls needs to focus on minimising moisture risk, in order to maintain the durability of the building and contribute to the national sustainable goals. Therefore, the IWI systems specification needs to ensure that the insulation materials do not damage the durability of the building structure.

Hygrothermal simulations can be used for specification by designers, construction practitioners and researchers. Monitoring each retrofit intervention requires time and resources; therefore, combining hygrothermal simulations and a scenario analysis can be a fast and inexpensive way to inform decision making – provided that simulations are representative of the hygrothermal behaviour of the component studied. Recent strategies for the conservation and retrofit of historic buildings are developed in dynamic simulation tools (10-13). The main tools are WUFI, DELPHIN and COMSOL Multiphysics, which are used for detailed numerical simulations to understand the moisture response of components and materials to boundary conditions. These tools have passed the HAMSTAD benchmark test, and most of them have been validated based on laboratory data (14-16). However, an inadequate assessment could lead to the specification of inappropriate IWI. Recently, researchers have started focusing on calibration methods for the hygrothermal simulations of internally insulated walls (17).

Calibration methods could be divided into manual and automatic. Many studies have examined the relationship between manual and automatic calibration methods. Taylor et al. (18) proved that the manual calibration method is more accurate than the automatic method, but automatic calibration is dominant in saving time and intelligent programming. For model calibration with limited parameters, manual calibration is more suitable (19).

The indicators of model calibration are critical to the evaluation of results. RMSE (Root Mean Square Error) and CVRMSE (Coefficient of Variation of RMSE) are used as standard statistical indicators (20). The related calculation formulas are shown in Equations [1] and [2], where s represents the simulation data, and m represents the monitoring data.

$$RMSE = \sqrt{\frac{\sum_{i=1}^{n}(s_i - m_i)^2}{n}} \qquad [1]$$

$$CVRMSE = \frac{RMSE}{m_{mean}} \times 100\% \qquad [2]$$

To perform the simulation, the modeller must assume some parameters. For instance, the hygrothermal properties of materials are unknown unless sampling and laboratory measurements are performed. A previous study suggested that model material properties could be imported from existing material libraries at the location of the building, if existing (21). Therefore, the stone properties input for solid walls simulation could be selected based on the details of the local stone.

2 Methodology

2.1 Case study building

A historic stone masonry building located in Edinburgh (Figure 1) was selected as the case building of this study (22). Over the past five decades, the rainfall in Scotland had always been maintained at a higher level than other areas in the UK (23). This case building is a two-level stone masonry building with a pitched roof used for wholesale and retail , which was built in 1850. The construction of this historic building is traditional, the exterior of the wall is composed of masonry and ashlar, and the interior of the wall is mainly lath and plaster. The U-values of the envelope structure were measured in-situ by HES, as shown in Table 1 (24).

Figure 1 – Case study building

Table 1 – Build-up and thermal transmittance of the exterior wall (25)

Materials	Thickness (mm)	U-value (W/(m^{2}K))
Outside - Craigleith Sandstone (with Lime Mortar)	500	
Blown Cellulose	50	
Inside - Lath and plaster	10	
Total		0.66

2.2 Baseline model

A one-dimensional baseline model was built in Delphin according to the built-up of the case study wall. The related parameter inputs are shown in Table 2. The exterior wall of the case study building consists of sandstone, mortar and a limited amount of rubble without a uniform structure of regular mortar joints and an unknown ratio of mortar to stone. This ratio for baseline models was assumed to be 3:7 (26).

Table 2 – Data for baseline model

Surface Properties	
Orientation	270°
Inclination	90°
Inside Surface	
Climate Conditions	Variables: Temperature (K) Related Humidity (%) Source: Case study building internal monitoring data
Boundary Conditions	Heat Conduction: Exchange coefficient for still air: 8 $\frac{kg}{ms^3K}$ Vapour Diffusion: Exchange coefficient for still air: 1×10^{-8} $\frac{s}{m}$
Outside Surface	
Boundary Conditions	Heat Conduction: Convective heat conduction exchange coefficient: 12 $\frac{kg}{ms^3K}$ Radiant heat conduction exchange coefficient: 5 $\frac{kg}{ms^3K}$ Effective heat conduction exchange coefficient: 12 $\frac{kg}{ms^3K}$ Vapour Diffusion: Vapour diffusion mass transfer coefficient: 7.5×10^{-8} $\frac{s}{m}$ Short-wave Solar Radiation: Solar absorption coefficient: 0.7 Long-wave Radiation Exchange: Long-wave emissivity: 0.9 Wind Driven Rain (EN ISO 15927-3): Reduction/Splash coefficient: 0.7
Initial Conditions	
Temperature	293 K
Relative Humidity	60%

The Delphin database hosts the hygrothermal properties of some materials. The properties of blown-in cellulose and lime plaster in Baseline models were input according to the database. The properties of sandstone and mortar were obtained by means of laboratory measurements of Scottish masonry materials (27). The type of sandstone was tested during calibration. Table 3 shows the properties and thickness input of mortar, cellulose and plaster. The baseline model is shown in Figure 2. The stone layer on the outside is assumed to be thicker than the inside at 200mm and 150mm, respectively. The thickness of the mortar is 150mm to meet the expected ratio (3:7).

Figure 2 – The one-dimensional baseline model in Delphin

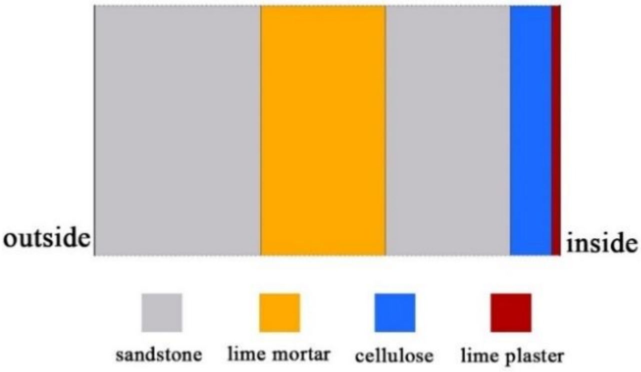

Table 3 – Hygrothermal properties for mortar, cellulose and plaster

Materials	Thickness [mm]	Thermal conductivity $\lambda\ [\frac{W}{mK}]$	Diffusion Factor $\mu\ [-]$	Moisture storage		Water absorption coefficient $A_w\ [\frac{kg}{m^2\sqrt{s}}]$	Porosity $\theta_{por}\ [\frac{m^3}{m^3}]$	Source
				W_{sat} $[\frac{kg}{m^3}]$	W_{80} $[\frac{kg}{m^3}]$			
Hot-mixed lime mortar	150	0.2	23	307	18	0.32	0.3	(27)
Blown-in cellulose	50	0.0482	2.0487	780	6.33	0.563	0.926	Delphin database
Lime plaster	10	0.82	12	285	11.06	0.127	0.302	Delphin database

2.3 Calibration of hygrothermal model

The calibration process selected the actual data by HES monitored between January 2019 and October 2019 as the target. The monitoring data contains the relative humidity and temperature at an interval of 15 minutes of the west-facing wall, measured within the first-floor wall. Sensors were located at different depths, namely 50mm (sensor 1), 100mm (sensor 2), 215mm (sensor 3) and 430mm (sensor 4) from the inner surface (Figure 3). The monitoring data was resampled using the mean into a set of one-hour intervals for subsequent simulations.

Figure 3 - Location of sensors for indoor conditions monitoring and in-wall monitoring (28)

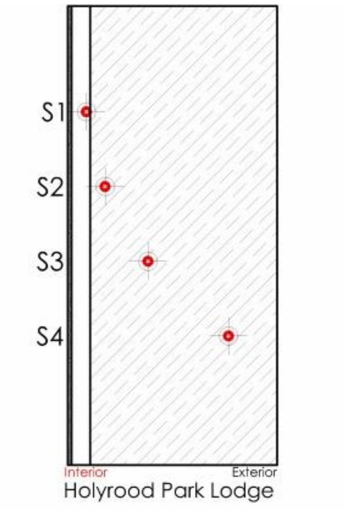

Each simulation generated the following results at the four depths considered in the monitoring, for the time between January 2019 and October 2019:

- Hourly Temperature (^{o}C)
- Hourly Relative Humidity (%)

The hourly temperature and relative humidity of each sensor were compared to the monitoring data of the same sensor by calculating the CVRMSE and evaluating it against the criteria set out in ASHRAE Guideline 14 (Table 4).

Table 4: ASHRAE Guideline 14 for calibration results (29)

Guideline	**Hourly Limit (%)**
CVRMSE	30

The calibration explores the model parameter inputs closest to the actual building to ensure that further scenario simulations are accurate and feasible. In this study, models were built in Delphin 6.1.1. Certain inputs were adjusted to make the simulation results close to the monitoring data. The calibration process was an iterative simulation, which contained four steps. A prevailing model, which has the smallest CVRMSE values that meet the criteria, was selected in each step as the baseline model for the next step. A total of ten simulations were performed in this iteration.

2.3.1 Step 1: Sandstone Type

This step compared the simulation results of the baseline model applied to five different sandstone types to explore a target stone that is most similar to the actual one. Krenzheimer sandstone, Velbke sandstone and Ruthen sandstone were selected from the Delphin database. Craigleith sandstone and Hailes sandstone were selected from Scottish materials data (27). Their properties are shown in Table 5. According to the results, Hailes sandstone has the closest results to the monitoring data, which was used for the following steps.

Table 5: Hygrothermal properties for sandstone

Materials	Thermal conductivity $\lambda\ [\frac{W}{mK}]$	Diffusion Factor $\mu\ [-]$	Moisture storage $W_{sat}\ [\frac{kg}{m^3}]$	Moisture storage $W_{80}\ [\frac{kg}{m^3}]$	Water absorption coefficient $A_w\ [\frac{kg}{m^2\sqrt{s}}]$	Porosity $\theta_{por}\ [\frac{m^3}{m^3}]$	Source
Krenzheimer sandstone	1.710	148.42	125	3	0.01	0.186	Delphin database
Velbke sandstone	1.83	11.474	242.23	1.561	0.646	0.267	Delphin database
Ruthen sandstone	2	12.976	244.58	14.2	0.338	0.276	Delphin database
Craigleith sandstone	1.7	120	45.2	10.5	0.0081	0.08	(27)
Hailes sandstone	1.9	63	89.5	6.2	0.036	0.13	(27)

2.3.2 Step 2: Model Dimension

In this step, the 2D model (Figure 4) was built with the sandstone selected in step. Except for the stone and mortar layer, other inputs are consistent with the baseline model. The results of the 2D model were compared with the monitored results of step 1 to explore the impact of model dimension on simulation results. According to the details of the case building, the height of a single stone was assumed to be 371mm. The thickness of the outside stone, mortar and inside stone was 250mm, 100mm and 150mm to achieve 3:7 of a ratio of mortar to sandstone.

Figure 4 – Two-dimensional model in Delphin

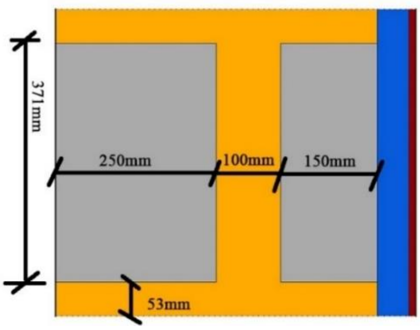

2.3.3 Step 3: Mortar-to-Stone Ratio

In this step, the mortar-to-stone ratio was changed (range 1:2 to 1:9). The simulation results of the larger ratio (1:2) and lower ratio (1:9) were compared with the monitored results of step 2.

2.3.4 Step 4: Insulation Material Thickness

There are many uncertainties in hygrothermal models of historical buildings, especially the thickness of materials. For instance, as the finish composed of lath and lime plaster contains some fine chips, they may mix into the insulating material during construction, resulting in a gap between the actual insulating material thickness and the design value. In this step, the insulation material (cellulose) was modified (±5mm) to explore the impact of insulation material thickness on calibration results.

2.4 Climate data for calibration

The 2019 hourly climate observations for Edinburgh and its surrounding stations were obtained from the MIDAS Open database for creating weather files (30). Due to incomplete data for one site, the collected data is assembled from different sites. The available variables from the MIDAS Open are shown in Table 6.

Table 6: Required parameters for weather files from MIDAS Open

<table>
<tr><th>Variables</th><th>Interval</th><th>Station</th><th>Unit</th></tr>
<tr><td>Air Temperature</td><td>1 hour</td><td rowspan="2">Edinburgh Royal Botanic Garden</td><td>℃</td></tr>
<tr><td>Relative Humidity</td><td>1 hour</td><td>%</td></tr>
<tr><td>Global Horizontal Irradiation</td><td>1 hour</td><td rowspan="3">Edinburgh Gogar bank</td><td>$\frac{kJ}{m^2}$ converted to $\frac{W}{m^2}$</td></tr>
<tr><td>Wind Direction</td><td>1 hour</td><td>° Clockwise from North</td></tr>
<tr><td>Wind Velocity</td><td>1 hour</td><td>$\frac{m}{s}$</td></tr>
<tr><td>Rain</td><td>1 hour</td><td rowspan="2">Edinburgh Royal Botanic Garden</td><td>mm</td></tr>
<tr><td>Dewpoint Temperature</td><td>1 hour</td><td>℃</td></tr>
<tr><td>Cloud Index</td><td>1 hour</td><td>Glasgow Bishopton</td><td>Oktas, converted to [0,1]</td></tr>
<tr><td>Direct Radiation Normal</td><td colspan="2" rowspan="2">Unavailable – Calculated by pvlib-python (31)</td><td rowspan="2">$\frac{W}{m^2}$</td></tr>
<tr><td>Diffuse Radiation Horizontal</td></tr>
<tr><td>Air Pressure</td><td colspan="2">Unavailable – Calculated from air temperature (32)</td><td>Pa</td></tr>
<tr><td>Long Wave Counter Radiation</td><td colspan="2">Unavailable – Calculated from air temperature, dewpoint temperature, air pressure and cloud index (33)</td><td>$\frac{W}{m^2}$</td></tr>
</table>

3 Results and discussions

3.1 Step 1: Sandstone Type

For the temperatures, the simulation results have a very similar trend as the actual data at all sensors locations, although with slightly lower values. The results of the five sandstones are highly close to each other because they have similar thermal properties (see Figure 5). This could be seen in the comparative analysis of the CVRMSE between simulation results and actual data (Table 7). For temperature, all CVRMSE results meet the ASHRAE 14 criterion. The calibration process is more concerned with relative humidity.

Figure 5: Simulation results of different sandstones and monitored temperature data, for sensor 2. Similar results were found for other sensor locations

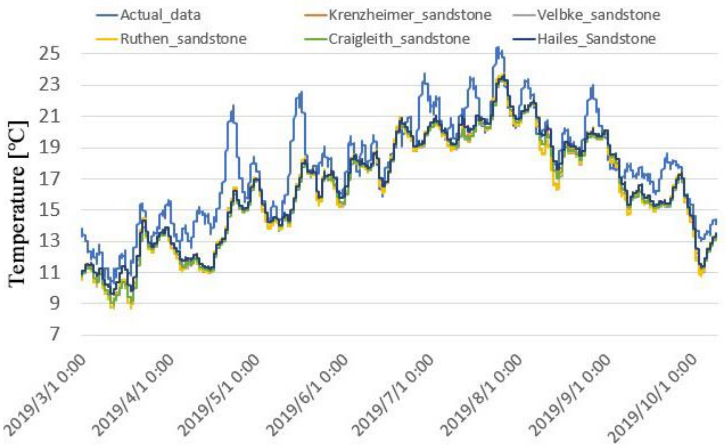

Table 7: CVRMSE of temperature results of different sandstones; lowest values of CVRMSE in bold

Sensors	CVRMSE [%]				
	Krenzheimer sandstone	Velbke Sandstone	Ruthen Sandstone	Craigleith Sandstone	Hailes sandstone
Sensor 1	15.00	15.54	15.36	15.31	**14.40**
Sensor 2	11.03	11.52	11.20	11.52	**10.58**
Sensor 3	10.83	11.21	10.84	11.30	**10.41**
Sensor 4	21.80	22.72	22.78	21.17	**20.94**

Figure 6 shows the variation trend of the relative humidity simulation results and actual data at the four sensors. For relative humidity, the simulation results are mostly higher than the actual data. The relative humidity curve of Hailes sandstone is always above the curves of other stones, which is closest to the actual data curve, and embodies a high degree of correlation. From the graphs, the results of other stones are irrelevant and incomparable with the actual data.

Sensor 1 is located in the insulating material layer of the model, which is close to the inside surface. The relative humidity at sensor 1 is similar across the five sandstones as the inside condition significantly impacts the results. However, the other three sensors are located in the sandstone and mortar layers, and their corresponding results have a large gap between different sandstones. Hailes and Velbke sandstone show more fluctuations in relative humidity. For the other sandstones, the relative humidity, especially at sensor 3 and sensor 4, rises rapidly at the beginning of the simulation and then remains stable.

Figure 6: Simulation results of different sandstones and monitored relative humidity data, at four sensors locations

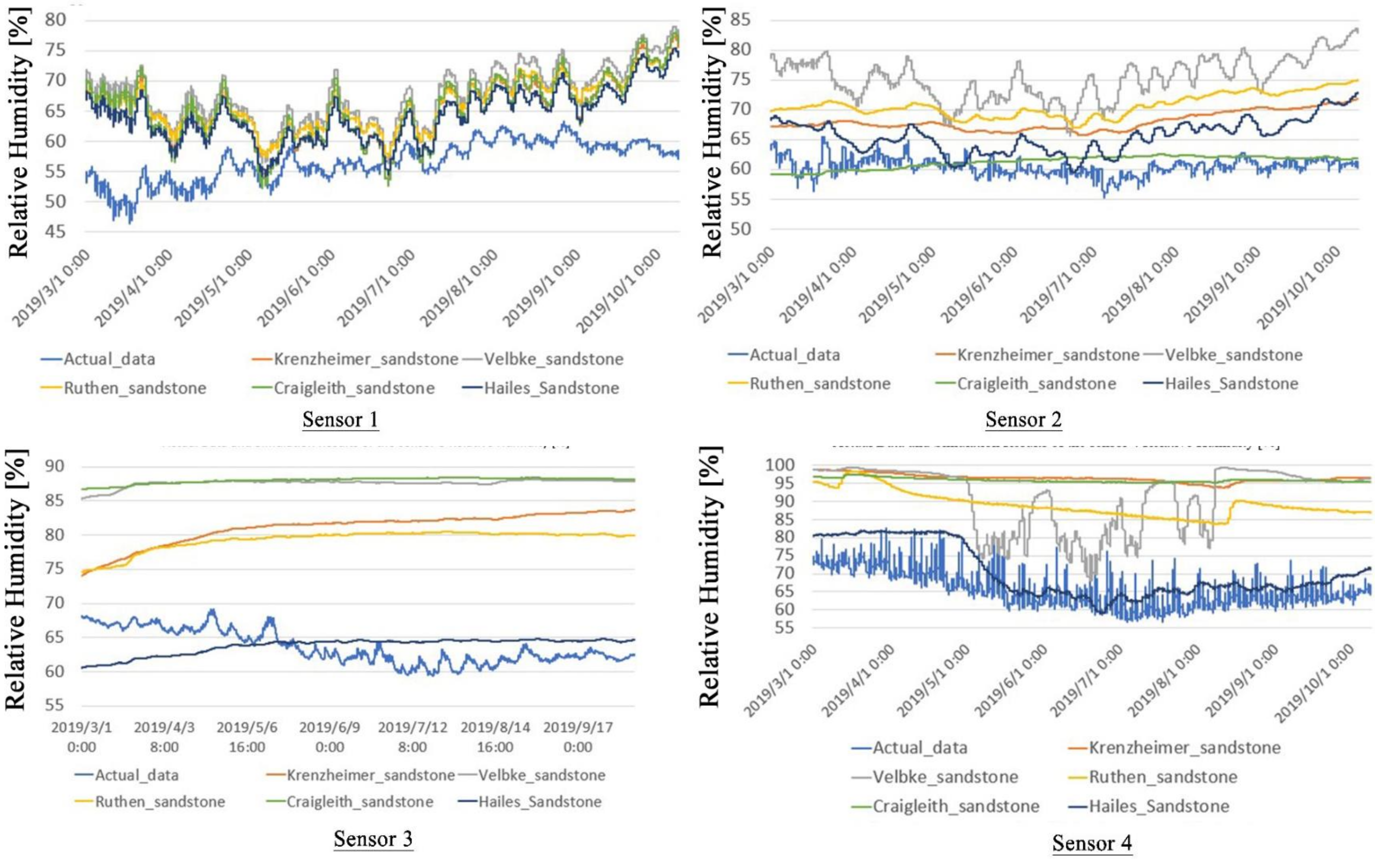

From Table 8, Hailes sandstone becomes the dominant stone type in the relative humidity simulation with the lowest CVRMSE at sensors 1, 3 and 4. Considering the temperature and humidity simulations comprehensively, Hailes sandstone has minor gaps in variation trends and errors from the monitoring data. Therefore, Hailes sandstone was selected for the final calibrated model.

Table 8: CVRMSE of relative humidity results of different sandstones; lowest values of CVRMSE in bold.

Sensors	CVRMSE [%]				
	Krenzheimer sandstone	**Velbke Sandstone**	**Ruthen Sandstone**	**Craigleith Sandstone**	**Hailes sandstone**
Sensor 1	20.10	23.97	21.01	20.65	**18.02**
Sensor 2	13.10	25.12	17.56	**3.71**	9.66
Sensor 3	28.48	38.11	25.49	38.74	**7.47**
Sensor 4	48.38	41.96	37.06	47.59	**10.26**

3.2 Step 2: Model Dimension

Figure 7 shows the relative humidity of 1D model, 2D model and monitoring data at sensor 1. The 1D model obtains closer results to the monitoring data than the 2D model in both temperature and relative humidity simulations. This phenomenon can also be observed in the results of other sensors and the CVRMSE (Table 9).

Figure 7: Simulation results of different model dimensions and monitored relative humidity data, for sensor 1

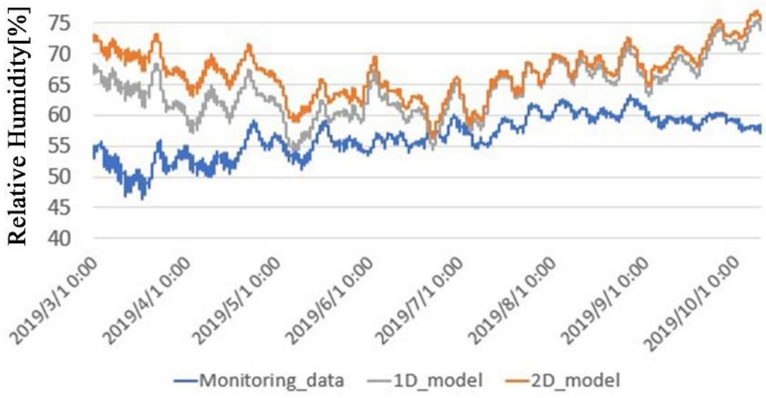

Table 9: CVRMSE of relative humidity results of different model dimensions

Sensors	CVRMSE [%]	
	1D model	2D model
Sensor 1	18.02	22.54
Sensor 2	9.66	18.59
Sensor 3	7.47	18.36
Sensor 4	10.26	19.63

The 1D model has closer results to monitoring data than the 2D model, possibly because of the influence of the vertical mortar representing a capillary break in the simulation. Although the layout of the mortar and sandstone of the 2D model is more similar to the actual construction, the simplified 1D model led to more representative results. Therefore, the 1D model was considered for the final model.

3.3 Step 3: Mortar-to-Stone Ratio (MSR)

Using relative humidity at sensor 1 as an example, Figure 8 illustrates the trend of relative humidity results of different MSR and monitoring data. From the graphs, the gap between simulation results and monitoring data is negatively correlated with MSR, which rise in MSR leads to more satisfactory results.

Figure 8: Simulation results of different mortar-to-stone ratios and monitored relative humidity data, for sensor 1

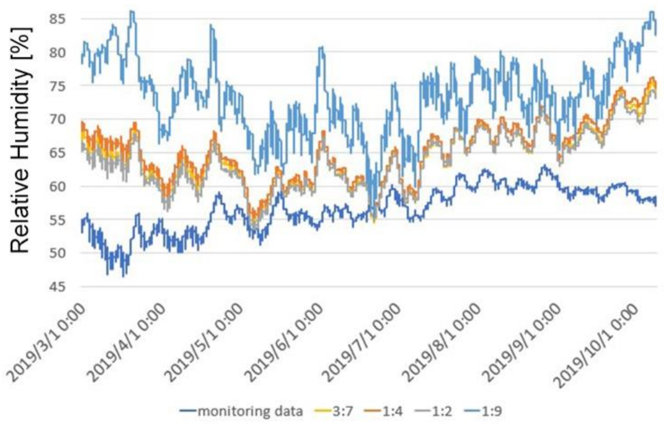

Table 10: CVRMSE of relative humidity results of different mortar-to-stone ratios

Sensors	CVRMSE [%]			
	1:9	1:4	3:7	1:2
Sensor 1	31.27	19.66	18.02	16.77
Sensor 2	26.35	10.97	9.66	8.55
Sensor 3	9.00	7.92	7.47	7.62
Sensor 4	18.62	12.70	10.26	9.50

According to Table 10, a decrease in MSR from 3:7 could cause the results to deviate from the monitoring data, suggesting the need for a capillary break in the hygrothermal model, here represented by a thicker layer of mortar. A rise in MSR from 3:7 made the results at most locations approach the monitoring data. Sensors 1 and 2 are closer to the critical surface than other sensors and were considered for the selection of MSR. Therefore, a mortar-to-stone ratio of 1:2 was selected for the next step.

3.4 Step 4: Insulation Material Thickness

Figure 9 shows the trend of the relative humidity results of different insulation material thicknesses and monitoring data at sensor 2. The insulation material thickness is positively correlated with the gap between simulation results and monitoring data. According to Table 11, reducing the insulating material thickness could improve the simulation accuracy for the central area of the model. Conversely, a rise in the insulating material thickness makes the simulation on the sides of the model more accurate. Since scenario simulations focused on the relative humidity of the critical surface (close to sensors 1 and 2), 55mm of insulation materials was selected for the final calibrated model.

Figure 9: Simulation results of different insulation material thicknesses and monitored relative humidity data for sensor 2

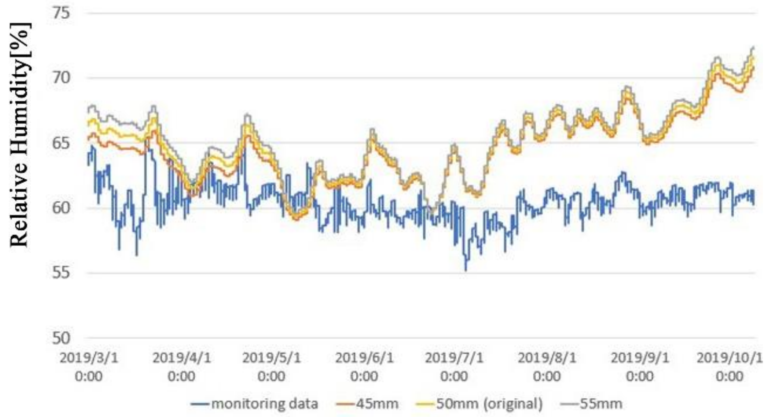

3.5 Final Calibrated Model

The materials and layout of the calibrated model (Figure 10) were determined by the calibration simulation results.

Figure 10: The calibrated model

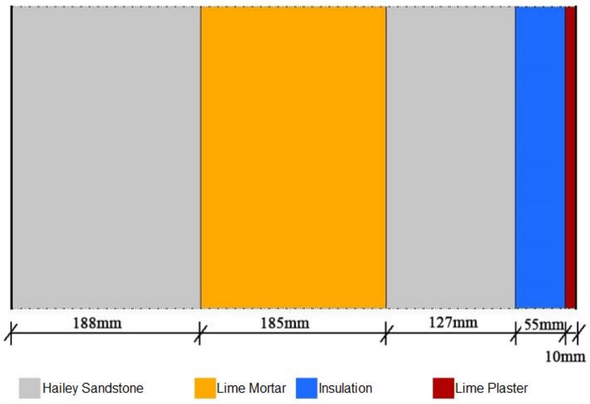

From the analysis of the CVRMSE results during calibration, the accuracy of the model largely depended on the selection of sandstone.

The error between simulation results and monitoring data saw the most fluctuating changes when testing different stones in hygrothermal calibration simulations. It is very reliable to select stone properties in the database that are geographically close to the case building. Other scholars also agreed with this finding (21). However, both Hailes sandstone and Craigleith sandstone are from Scotland and saw a different behaviour in the simulations. Therefore, selecting local material properties as input is only part of the success; in this case, the calibration exercise was able to support the final material selection.

4 Conclusions

Internal wall insulation is a possible solution for protecting the façade of historic buildings while saving energy, improving indoor thermal comfort, and reducing carbon emissions. However, an inadequate assessment could lead to the specification of inappropriate IWI, affecting the durability of the wall. Scenario analysis by means of hygrothermal simulations is a useful method to explore suitable assemblies to participate in retrofit or design schemes of buildings. Calibration is one of the essential parts of the simulation, which improves the accuracy and representativeness of simulation results.

To explore the impact of the calibration of hygrothermal simulations on the retrofit of solid walls, this paper used a case study to perform hygrothermal simulations in Delphin. The calibration simulations were divided into four steps, which respectively test the influence of sandstone type, model dimension, MSR, and insulation material thickness on the simulation results. The required simulations were completed under the current weather. The current climate data was established based on the MIDAS Open dataset. The following are the main results:

- The temperature simulations showed more stable and accurate results than relative humidity.
- Appropriate calibration could effectively improve the accuracy of relative humidity simulations, which highly depends on the adjusted parameters.

- The sandstone type (material properties input) was the most critical factor, if compared with model dimension, mortar thickness and mortar-to-stone ratio - as long as a capillary break is considered in the model.

The calibrated model can be used as a reference model for scenario simulations to explore the best refurbished assembly.

In the future research, field trips and detailed confirmation of case building could be implemented to obtain more accurate parameter settings for modelling. Besides, databases of more new weather observatories are worth exploring to bring simulations closer to reality.

References

(1) IEA, World Energy Balances: Overview, OECD/IEA, 2018.

(2) IEA, *CO2 Emissions from Fuel Combustion Highlight 2017*, OECD/IEA, 2017.

(3) The Guardjan , Number of new UK homes registered to be built hits 13-year high, *Construction Industry*, 2020. Retrieved March 02, 2022, from https://www.theguardian.com/business/2020/feb/06/number-of-new-uk-homes-registered-to-be-built-hits-13-year-high.

(4) Department for Communities and Local Government, *Technical Report, English Housing Survey,* Headline Report, 2017, vol. 8010.

(5) DEFRA, *Energy analysis focus report a study of hard to treat homes using the English house condition survey*, Department of Environment and Rural Affairs, 2008.

(6) Zhou, X., Derome, D., and Carmeliet, J., Hygrothermal Modeling and Evaluation of Freeze-thaw Damage Risk of Masonry Walls Retrofitted with Internal Insulation*, Building and Environment*, 2017, 125: 285-298.

(7) Netinger Grubeša, I., Teni, M., Krstić, H. and Vračević, M., Influence of Freeze/Thaw Cycles on Mechanical and Thermal Properties of Masonry Wall and Masonry Wall Materials*, Energies*, 2019, 12(8).

(8) Hao, L., Herrera-Avellanosa, D., Del Pero, C., Troi, A. What Are the Implications of Climate Change for Retrofitted Historic Buildings? A Literature Review. *Sustainability* 2020, 12(18):7557.

(9) Taoukil, D., Sick, F., Mimet, A., Ezbakhe, H., and Ajzoul, T., Moisture content influence on the thermal conductivity and diffusivity of wood–concrete composite, *Construction and Building Materials*, 2013, 48:104–115.

(10) Webb, A. L., Energy retrofits in historic and traditional buildings: A review of problems and methods, *Renewable and Sustainable Energy Reviews*, 2017, 77, pp. 748-759.

(11) Akkurt, G. G., et al. Dynamic thermal and hygrometric simulation of historical buildings: Critical factors and possible solutions, *Renewable and Sustainable Energy Reviews*, 2020, 118.

(12) Jensen, N. F., et al., Hygrothermal assessment of four insulation systems for interior retrofitting of solid masonry walls through calibrated numerical simulations, *Building and Environment*, 2020, 180.

(13) Bottino-Leone, D., Larcher, Marco, Troi, Alexandra, and Grunewald, John., Hygrothermal characterization of a fictitious homogenized porous material to describe multiphase heat and moisture transport in massive historic walls, *Construction and Building Materials*, 2021, 266.

(14) Knarud, J.I. and Geving, S., Implementation and benchmarking of a 3D hygrothermal model in the COMSOL multiphysics software, *Energy Procedia*, 2015, 78: 3440–3445.

(15) Maliki, M., Laredj, N., Naji, H., Bendani, K., Missoum , H., Numerical modelling of hygrothermal response in building envelopes. *Gardevinar*, 2014, 66 (11): 987–995.

(16) Sontag, L., Nicolai, A., and Vogelsang, S. Validierung der Solverimplementierung des hygrothermischen Simulationsprogramms DELPHIN, 2013.
(17) Panico, S., Larcher, M., Troi, A., Codreanu, I., Baglivo, C., Congedo, P.M., Hygrothermal analysis of a wall isolated from the inside: the potential of dynamic hygrothermal simulation, *IOP Conference Series: Earth and Environmental Science*, 2021, 863: 012053
(18) Taylor, D.A.A., Pawar, V., Kruzikas, D, Gilmore, K.E., Pandya, A., Iskandar, R., and Weinstein, M.C. Methods of Model Calibration - Observations from a Mathematical Model of Cervical Cancer, Pharmacoeconomics, 2010, 28(11): 995-1000.
(19) Im, P. and Bhandari, M., Is monthly and whole building level calibration enough? - A detailed modeling and calibration study of an ultra-efficient occupancy simulated house. *In ASHRAE/IPBSA-USA Building Simulation Conference*,2014, pp. 177-186.
(20) Cornaro, C., Bosco, F, Lauria, M, Puggioni, V, and Santoli, L., Effectiveness of Automatic and Manual Calibration of an Office Building Energy Model, *Applied Sciences*, 2019, 9 (10): 1985.
(21) Adhikari, R.S., Lucchi, E., and Pracchi, V.N, Experimental measurements on thermal transmittance of the opaque vertical walls in the historical buildings, *In 28th Conference, Opportunities, Limits & Needs Towards an environmentally responsible architecture,* 2012, Lima, Peru.
(22) Historic Environment Scotland, Refurbishment Case Study 37 - Holyrood Park Lodge, Edinburgh: Thermal upgrade works to a 19th century lodge house, 2020. Retrieved March 2, 2022, from https://www.historicenvironment.scot/archives-and-research/publications/publication/?publicationid=f7c8b362-f78b-416a-9733-abb5009c521d
(23) Jones, M. R., Fowler H.J., Kilsby C.G., Blenkinsop S., An assessment of changes in seasonal and annual extreme rainfall in the UK between 1961 and 2009, *International Journal of Climatology*, 2013, 33(5): 1178-1194.
(24) Historic Environment Scotland, Condition Survey Report, *Technical report*, 2016. Retrieved August 19, 2021, from https://www.hiberatlas.com/smartedit/projects/120/Condition%20Survey%20Report.pdf.
(25) *Hiberatlas, Holyrood Park Lodge*. Retrieved August 19, 2021, from https://www.hiberatlas.com/en/holyrood-park-lodge--2-120.html
(26) Baker, P., U-values and traditional buildings In situ measurements and their comparisons to calculated values, *Historic Scotland Technical Paper 10*, 2011, Glasgow Caledonian University.
(27) Banfill, P.F.G., Hygrothermal simulation of building performance: data for Scottish masonry materials, *Materials and Structures,* 2021, 54(4).
(28) Archimetrics Limited, Observations Report 5: U-value, Wall & Room Conditions. Holyrood Park Lodge: Refurbished. *Technical report*, 2019.
(29) ASHRAE Guideline 14. Measurement of Energy and Demand Savings, ASHRAE, 2002, Atlanta, GA, USA.
(30) Met Office, Met Office MIDAS Open: UK Land Surface Stations Data (1853-current). *Centre for Environmental Data Analysis*, 2019. Retrieved 21 December 2021, from http://catalogue.ceda.ac.uk/uuid/dbd451271eb04662beade68da43546e1
(31) *Pvlib Python*. Retrieved August 19, 2021, from https://pvlib-python.readthedocs.io/en/latest/package_overview.html#package-overview.

(32) Casio Computer, *Atmospheric pressure from altitude calculator*. Retrieved August 19, 2021, from https://keisan.casio.com/exec/system/1224579725.
(33) Kehrer, M., *WUFI Workshop NBI / SINTEF 2008 Radiation Effects On Exterior Surfaces*. Retrieved August 19, 2021, from https://pdfs.semanticscholar.org/cccb/9b35c72d14e701008f84b55cb085850d4a15.pdf.

Acknowledgements

The authors would like to acknowledge the support of Caroline Rye and Cameron Scott of ArchiMetrics Ltd and Prof Phil Banfill at Heriot-Watt University for providing the data used in this study.